The Application of Velocity Decomposition to Airfoil Problems

William J. Rosemurgy†, Kevin J. Maki, and Robert F. Beck

Department of Naval Architecture and Marine Engineering
University of Michigan, Ann Arbor, MI, 48109 USA
[brosemu, kjmaki, rbeck]@umich.edu

† Presenting Author

Introduction

The work presented in this paper is the continuation of work previously presented at the IWWWFB by Edmund et al. (2011). The goal of this research is to find a method that provides the solution in the entire fluid domain of the Navier-Stokes problem, while being more computationally efficient than existing methods that require full field discretization. To achieve this goal, we use a velocity decomposition where the total velocity vector is expressed as the sum of an irrotational component and a vortical component. The majority of the flow in the fluid domain is irrotational and can be expressed as the gradient of a potential field. Rotational flow will be confined to the boundary layer near the body, the wake region downstream of the body, and the turbulent regions associated with breaking waves. It is well known that the potential which satisfies a zero-normal flow condition on the body (the *inviscid* potential) does not satisfy the real viscous flow problem even in the regions away from the body where the flow is essentially irrotational. This is almost entirely due to viscous effects near the body. Therefore, we seek a formulation for the *viscous* potential which incorporates the effects of viscosity in a general manner.

The work in Edmund (2012) applied velocity decomposition to the steady, non-lifting flow over deeply-submerged bodies at a wide range of Reynolds numbers. The ultimate goal of the current research is to apply our approach to free-surface problems. The flow over a body under a free surface is almost always asymmetrical which presents challenges for our approach. To address these issues we began by investigating the steady flow over a 2-dimensional, deeply-submerged NACA0012 airfoil which also has an asymmetrical velocity field around the body and in the wake. It is expected that the results presented at the Workshop will include a free surface, and a comparison to Duncan's experiments (1983) will be made.

Velocity Decomposition

We seek a velocity decomposition that provides a potential field which satisfies the real fluid problem in the region of space where the total velocity has no rotation. To arrive at a formulation for the viscous potential, we start with the decomposition of the total velocity vector, $\mathbf{u}$, as the sum of the gradient of the viscous potential, $\nabla\varphi$, and a vortical component, $\mathbf{w}$.

$$\mathbf{u} = \nabla\varphi + \mathbf{w} \tag{1}$$

If a viscous potential is found that delivers a vortical velocity field which vanishes with the vorticity vector, then the total velocity can be described completely by the gradient of the viscous potential outside of the vortical regions.

$$\mathbf{u} = \nabla\varphi \tag{2}$$

This opens the possibility to solve the governing equations for the viscous flow (Navier-Stokes, Reynolds-averaged Navier-Stokes, etc.) on a reduced fluid domain and to use the gradient of the viscous potential as a Dirichlet condition on the outer boundary of this reduced discretization. With this approach, the reduced fluid domain only needs to contain the regions where the vortical velocity is non-zero.

As mentioned in the introduction, the viscous potential, φ, is different from the inviscid potential, ϕ. The inviscid potential satisfies the kinematic condition of zero normal flow on the body, while the viscous potential will satisfy a modified Neumann boundary condition that is not necessarily zero on the body. To derive this condition we start with the no-slip body boundary condition that the total velocity vector must satisfy.

$$\mathbf{u} = 0 = \mathbf{w} + \nabla\varphi \qquad \text{on the body} \tag{3}$$

or

$$\nabla\varphi = -\mathbf{w} \qquad \text{on the body} \tag{4}$$

Dotting both sides with the body normal vector we obtain:

$$\frac{\partial \varphi}{\partial n} = -\mathbf{w} \cdot \mathbf{n} = -w_n \text{ on the body} \tag{5}$$

Following Morino (1986), we use the principle of conservation of mass to obtain an expression for the rotational contribution to the body boundary condition for the viscous potential. The divergence operator and the vortical velocity are expressed in a local coordinate system consisting of a normal vector $\mathbf{n}$ and two in-plane tangent vectors, $\mathbf{t}_1$ and $\mathbf{t}_2$. If the total velocity is solenoidal and the viscous potential satisfies the Laplace equation then the divergence of the vortical velocity must be zero:

$$\nabla \cdot \mathbf{u} = \nabla \cdot \mathbf{w} + \underbrace{\nabla^2 \varphi}_{=0} = \nabla \cdot \mathbf{w} = \frac{\partial w_n}{\partial n} + \frac{\partial w_{t_1}}{\partial t_1} + \frac{\partial w_{t_2}}{\partial t_2} = 0 \tag{6}$$

This equation is then integrated in the normal direction out to a distance δ.

$$w_n(0) = \int_0^\delta \left[\frac{\partial w_{t_1}}{\partial t_1} + \frac{\partial w_{t_2}}{\partial t_2} \right] dn + w_n(\delta) \tag{7}$$

The result is the expression for the normal component of the vortical velocity on the body surface. Combining Equations 5 and 7 results in the body boundary condition for the viscous potential.

$$\frac{\partial \varphi}{\partial n} = -\int_0^\delta \left[\frac{\partial w_{t_1}}{\partial t} + \frac{\partial w_{t_2}}{\partial t_2} \right] dn - w_n(\delta) \text{ on the body} \tag{8}$$

We seek a decomposition in which the vortical velocity vanishes with the vorticity as one moves away from the body (in a normal direction). This means that for a distance δ that lies far enough away from the body such that the vorticity is negligible, the decomposition will provide a vortical velocity which is zero at δ. Consequently, Equation 9 gives the body boundary condition for the viscous potential.

$$\frac{\partial \varphi}{\partial n} = -\int_0^\delta \left[\frac{\partial w_{t_1}}{\partial t} + \frac{\partial w_{t_2}}{\partial t_2} \right] dn \text{ on the body} \tag{9}$$

We use Equation 2 to specify the Dirichlet condition for the viscous flow on the inlet and lateral (far-field) boundaries of a reduced computational domain. However, from Equation 9 it is apparent that knowledge of the vortical velocity is required in order to calculate the body boundary condition. We approach this with an iterative strategy. The inviscid potential is initially used to set the Dirichlet condition for the viscous flow. Then the solver iterates between the viscous flow solver and the potential solver until a converged solution is reached. The vortical velocity at δ, $w_n(\delta)$, in Equation 8 is initially non-zero but is driven to zero as a consequence of the iterative scheme.

The vortical velocity evolves in the wake downstream of the body. A source distribution downstream of the body is used in order to include the effects of the vortical wake. The source distribution in the wake also satisfies Equation 9.

Potential Flow Solver

We solve the viscous potential problem using a boundary element method satisfying the body boundary condition for the viscous potential given in Equation 9 as well as the far-field radiation condition. We use a combination of flat, 2-dimensional source and vortex panels. The vortex panels have a linearly varying strength while the source panels have constant strength. The Kutta condition is met by requiring the vortex strength at the trailing edge to be zero. In the usual manner, a system of linear equations is developed to solve for the unknown vortex strengths by collocating at the center of each panel and satisfying the inviscid zero normal flow velocity condition. Similarly, the unknown source strengths are determined by forming a separate system of linear equations by collocating at the center of each panel and satisfying the body boundary condition for the viscous potential from Equation 9. The systems are directly solved using LAPACK, an open-source linear algebra package.

The lifting problem introduces a new challenge that we have not encountered before. In previous work we have only dealt with non-lifting bodies where the body is symmetric with respect to the onset flow which results in a symmetric flow around the body as well as a symmetric wake downstream. We include the vortical effects of the symmetric wake by placing a source distribution from the trailing edge to the end of the computational

domain. However, in a lifting problem the vortical wake is not symmetric and we must adjust our model to include this asymmetry. To do this we use two source distributions separated by a small distance, usually less than 1% of the chordlength which is illustrated in Figure 1. The boundary condition for the upper wake source distribution integrates the vortical velocity in the positive vertical direction while the boundary condition for the lower wake source distribution integrates the vortical velocity in the opposite direction. The non-physical source distributions in the wake region cause no difficulty because the velocities due to the viscous potential are only evaluated outside of the rotational region of the flow.

Viscous Flow Solver

The viscous fluid equations are solved using OpenFOAM, a finite-volume, open-source CFD package. The steady fluid equations are solved using the SIMPLE algorithm. The Spalart-Allmaras turbulence model with wall functions is used when needed. It is also important to mention that the potential flow panel method uses the same discretization of the body as the viscous flow solver.

Results

Results are computed for a deeply-submerged NACA0012 airfoil at $0-7^\circ$ angles of attack. Since a comparison with Duncan's experiments (1983) is the ultimate goal, we use a Reynolds number of 160,000 and a chordlength of 0.202 m. The velocity decomposition result is computed on a reduced size grid which has inlet and lateral (far-field) boundaries at 5 chordlengths from the body with 27k cells. For comparison, a conventional RANS result is computed on a grid with boundaries located at 100 chordlengths with 44k cells. To be consistent the two domains share the same geometry in overlapping regions and both have downstream boundaries located 250 chordlengths downstream. The surface of the airfoil is discretized into 100 flat panels. Velocity profiles at the quarter-chord, mid-chord, trailing edge and one chordlength downstream are shown in Figures 3 and Figures 4 for angles of attack of 3° and 7°, respectively. The velocity decomposition result has excellent agreement with the RANS calculation on the large domain. Figure 2 shows the lift coefficient calculated from the RANS result across a range of angles of attack. Experimental values from Jacobs and Sherman (1937) are included in Figure 2 for a slightly higher Reynolds number of 170,000. Again, the agreement between the large domain result and the velocity decomposition is very good, within 0.25%

Conclusion

Our velocity decomposition approach has been successfully applied to solve for the real viscous flow over a deeply submerged NACA0012 airfoil. The next step is to include free-surface effects. We expect to present results for the free-surface flow over a NACA0012 airfoil at the Workshop.

Acknowledgements

The authors would like to gratefully acknowledge the support of grants from the US Office of Naval Research, Award #N00014-10-1-0301 under the technical direction of Ms. Kelly Cooper, as well as Awards #N00014-11-1-0484 and #N00014-09-1-0978 under the technical direction of Dr. L. Patrick Purtell.

Bibliography

Duncan, J. The breaking and non-breaking wave resistance of a two-dimensional hydrofoil. *Journal of Fluid Mechanics*, 126:507–520, 1983.

Edmund, D. O., Maki, K. J., and Beck, R. F. An improved viscous / inviscid velocity decomposition method. In *International Workshop on Water Waves and Floating Bodies (IWWWFB)*, volume 26, 2011.

Edmund, D. *A Velocity Decomposition Method for Efficient Numerical Computation of Steady External Flows*. PhD thesis, University of Michigan, 2012.

Jacobs, E. N. and Sherman, A. Airfoil section characteristics as affected by variations of the Reynolds number. Technical Report 586, National Advisory Committee for Aeronautics, 1937.

Morino, L. Helmholtz decomposition revisited: vorticity generation and trailing edge condition. *Computational Mechanics*, 1(1):65–90, 1986.

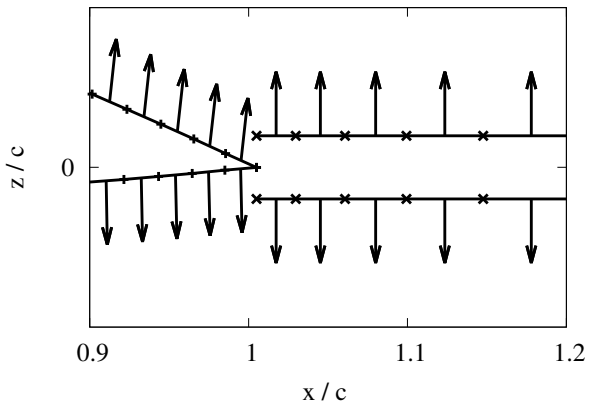

Figure 1: This figure shows the trailing edge region in order to describe the two wake surfaces.

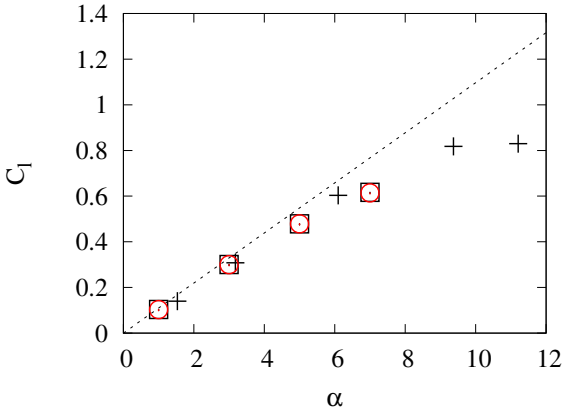

Figure 2: Lift coefficient vs. angle of attack. Thin wing theory (...), Experiments at Re = 170k by Jacobs and Sherman (1937) (+), Velocity decomposition (□), and Large domain RANS (○).

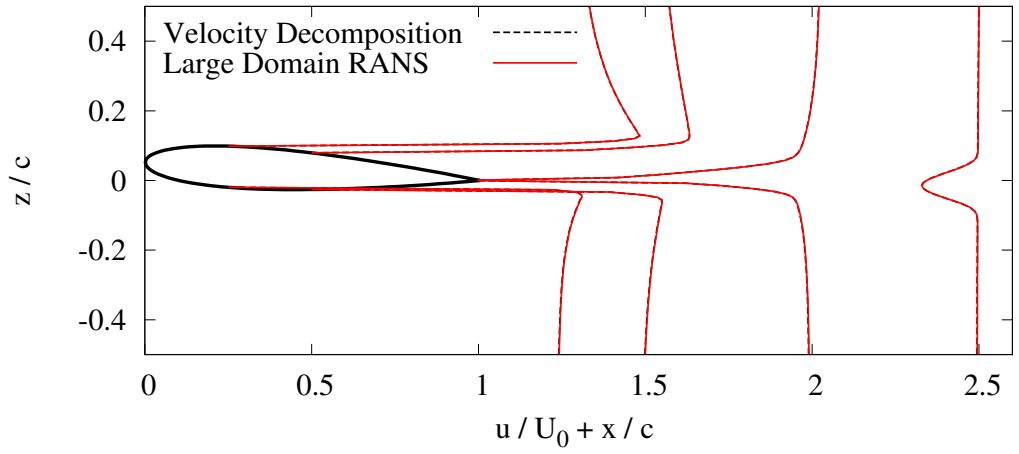

Figure 3: Velocity profiles calculated for a NACA0012 airfoil at 3° angle of attack computed using velocity decomposition, compared to the large domain (RANS) result.

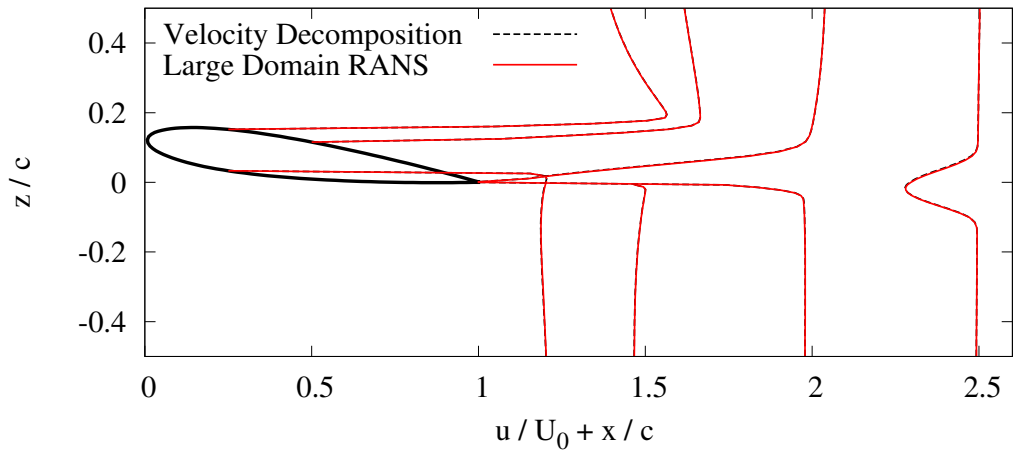

Figure 4: Velocity profiles calculated for a NACA0012 airfoil at 7° angle of attack computed using velocity decomposition, compared to the large domain (RANS) result.